Efficient and simultaneous immobilization of fluoride and lead in water and tea garden soil by bayberry tannin foam loaded zirconium

Xiaolu Huang
Sichuan Normal University
Mei Zhang
Sichuan Normal University
Minghui Wang
Sichuan Normal University
Zhuoyu Wen
Sichuan Normal University
Yamei Jiang
Sichuan Normal University
Yunhao Sui
Sichuan Normal University
Xiaoting Li
Sichuan Normal University
Jun Ma
Sichuan Normal University
Yang Liao (liaoyang79@sicnu.edu.cn)
Sichuan Normal University

Research Article

Keywords: compound pollution of tea, simultaneous immobilization of fluoride and lead, adsorption, morphological changes, tea garden soil

Posted Date: May 10th, 2023

DOI: https://doi.org/10.21203/rs.3.rs-2901197/v1

Abstract

Human activities have led to various pollution in the environment, and the combined pollution of fluoride and lead in acidic tea garden soil has received much attention. The key to eliminating this combined pollution is to immobilize pollutants simultaneously, thus preventing their migration from tea garden soil to tea trees. In this paper, the natural product bayberry tannin was employed as raw material to fabricate functional materials (TF-Zr) for simultaneous adsorption of fluorine (F) and lead (Pb) in water and soil by the reactivity of tannin with Pb^{2+} and the affinity of Zr with F. The characterization techniques such as SEM-Mapping, EDS, FT-IR, XPS were utilized to probe the adsorption mechanism. The results showed that TF-Zr could simultaneously and efficiently adsorb F^- and Pb^{2+} with the adsorption capacity of 5.02 mg/g (Pb) and 4.55 mg/g (F), and the adsorption processes were both in accordance with the proposed secondary kinetic adsorption model. Besides, the presence of F^- promoted the adsorption of Pb^{2+} by TF-Zr. The materials were applied into the tea garden soil to explore its effect on the variation of F and Pb forms in tea garden soil. It was found that the proportion of water-soluble fluorine, exchangeable fluorine and exchangeable lead in the tea garden soil decreased significantly, while the proportion of residual fluorine and residual lead increased evidently, illustrating TF-Zr possessed eximious fixation effect on the highly reactive fluorine and lead in the soil and facilitated their conversion to the more stable residue state. Therefore, TF-Zr can be used for the efficient and simultaneous immobilization of fluorine and lead in water and tea garden soil.

1. Introduction

With the intensification of human activities, various pollutants have entered the environment one after another, causing serious environmental pollution in water and soil (Havugimana et al. 2017). More seriously, the pollution has changed to combined pollution, which is mainly manifested by heavy metals, other inorganic and organic pollutants (Luo et al. 2021; Peng et al. 2021). Recently, the combined pollution of fluorine and lead in tea garden soil is particularly prominent in China. Qin et al. found that the average value of total fluorine content in a tea garden soil in China was 945 mg/kg, which was higher than the national average value of total soil fluorine (Qin et al. 2014). Guo et al. tested 150 tea gardens in Fujian Province, China, for soil heavy metals and found that 70% of the tea gardens had soil lead levels exceeding the organic tea garden limit (NY 5199 – 2002) (50 mg kg^{-1}) (Guo et al. 2011). As the tea tree grows, fluorine and lead in soil can be enriched in tea leaves (Long et al. 2021; Sun et al. 2020). Various diseases in human bodies may caused by drinking tea polluted by lead and fluorine (Cao et al. 1997; Zhuang et al. 2022). Research has shown that the absorption of heavy metals and fluorine by tea trees comes from water in soil (Gao et al. 2012; Zhang et al. 2020; Zhang et al. 2021). Meanwhile, the bioavailability of fluoride and lead is greatly increased in acidic tea plantation soils (Jin et al. 2005; Xu et al. 2022; Yang et al. 2018), which also potentially increases the migration of fluoride and lead from soil to tea tree and into human body through the food chain (Han et al. 2006; Ruan et al. 2003). Therefore, achieving the immobilization of lead and fluorine in water and soil is the key to solving the combined

pollution of fluorine and lead in tea garden soil, which is of great significance for soil ecology and human health and safety.

The addition of chemical stabilizers is one of the most common means of reducing the bio-availability of lead and fluorine in soil. For example, aluminum humate prepared by Huang et al. was able to significantly reduce the water-soluble fluorine content in tea plantation soil (Huang et al. 2020). Different charcoals reported by Gao could also effectively reduce the content of water-soluble and exchangeable fluorine in soil, which in turn significantly reduced the accumulation of fluorine in tea plants (Gao et al. 2012). Biochar loaded with iron lanthanides (BC/Fe-La) and aluminum lanthanides (BC/Al-La) prepared by Fan et al. were able to reduce water-soluble fluorine in soil by 87.58% and 90.17%, respectively (Fan et al. 2022). Chemical stabilizers can also change the morphology of heavy metal Pb and reduce the ionic mobility and bioavailability of Pb. For example, Zhang and Xia et al. achieved in situ immobilization of Pb in soil by preparing a chemical stabilizer(Xia et al. 2021; Zhang et al. 2022). The MgO-loaded fish scale biochar (MgO-FB) prepared by Qi et al was effective in immobilizing Pb and other heavy metals in soil (Qi et al. 2022). Although a series of chemical stabilizers have been developed for controlling fluorine or heavy metal Pb contamination in soils, few efficient chemical stabilizers have been reported for using in the combined contamination of fluorine and Pb in acidic tea garden soil, meanwhile reducing the biological effectiveness of fluorine and Pb. Plant tannins are natural and easily extractable polyphenols that can chelate with various heavy metal ions (Xu et al. 2017). However, tannin molecules are unstable and need to be modified when used as heavy metal adsorbents. In addition, Zr (IV) is highly electropositive and it shows excellent affinity for the highly electronegative F^- (Wang et al. 2014). Both Singh et al and Liu et al. reported that Zr (IV) is able to complex with F (Liu et al. 2013; Singh et al. 2020). Cho et al prepared hydrated zirconia chitosan bead composites, which were able to achieve simultaneous adsorption of fluorine and lead in aqueous solutions, but the adsorption efficiency needs to be improved, and the effect of its application in soil has not been explored (Cho et al. 2016).

Therefore, in this paper, the natural product poplar tannin was used as raw material to prepare functional materials for simultaneous immobilization of fluorine (F) and lead (Pb) by using the efficient chelation of tannin with Pb and the strong affinity of Zr with F. Firstly, the adsorption properties of the prepared materials on F^- and Pb^{2+} and their influencing factors were investigated in aqueous solution, and the mechanism of the adsorption of F^- and Pb^{2+} by the materials was revealed. Then, the material was applied to tea garden soil to investigate its stabilization effect on F and Pb in tea garden soil. This study may provide new ideas for the management of the combined pollution of fluorine and heavy metal Pb in water and soil, and provide guidance for reducing the biological effectiveness of fluorine and Pb in tea garden soil. The strategy and principle are shown in Fig. 1.

2. Experimental

2.1 Materials.

Bayberry tannin was purchased from Guangxi Rubber Factory. $Zr(SO_4)_2{\cdot}4H_2O$, NaF, hexamine, toluene-4-sulfonic acid, Tween80, $NaHCO_3$, HNO_3, urea, trisodium citrate, potassium dihydrogen phosphate, potassium chloride, lead nitrate, magnesium chloride, sodium acetate, hydroxylamine hydrochloride, hydrogen peroxide, ammonium oxalate, lead standard solution and fluorine standard solution were obtained from China Kolon Chemical, of which lead standard solution and fluorine standard solution are national standard substance reagents, and the rest of the drugs are of analytical grade.

2.2 Preparation of TF.

In a typical synthesis process, 40.00 g of tannin powder was dissolved in 60 mL of distilled water with 2 hours of stirring at ambient temperature. Then, 2.84 g of hexamine was added as the crosslinker while 1.12 g of toluene-4-sulfonic acid was as the catalyst. After stirring for 10 min, 1 mL of Tween80 was appended and the mixture was consequently stirred at 1800 $r{\cdot}min^{-1}$ for 1 h. In the end, the obtained mixture was cured at 85℃ for 24 h to gain brown tannin foam (TF).

2.3 Preparation of TF-Zr.

Above all, 2.00 g of $Zr(SO_4)_2{\cdot}4H_2O$ was dissolved in 100 mL of distilled water. 1.00 g of as-prepared TF material was consequently added following with 4 hours of stirring at 30℃. Then 7% $NaHCO_3$ was added dropwise to adjust the solution pH to 2–3 within 2 h, followed by continuous reaction at 40℃ for 1–2 h until the solution pH changed to 1.28–1.30. The obtained material was centrifuged at 4000 $r{\cdot}min^{-1}$ for 10 min, filtered, and the solid material was collected. It was washed repeatedly with deionized water and dried overnight at 40℃ under vacuum to obtain TF-Zr.

2.4 Characteristics of the materials.

SEM (FEI/quanta250) was used to observe the surface morphology of the materials, XPS (Shimadzu 119 ESCA-850) was utilized to characterize the electron binding energy of elements in materials. FTIR spectra (VERTEX 70) was applied to analyze the functional groups of the materials. The surface atomic composition of the adsorbent was examined by scanning electron microscopy (S-3400N Hitachi) and EDS techniques.

2.5 Adsorption of Pb^{2+} and F^{-}.

To investigate the adsorption capacity of TF-Zr on F^- and Pb^{2+}, different batches of TF-Zr dosage (0.02–0.12 g), the pH of solution (pH = 2.5-7), temperature (25℃-45℃) and different concentration ratios of Pb^{2+}: F^- (10:2, 10:5, 10:10, 10:15, 10:20, 10:30, 10:40, 10:50) were all studied, which explored the effect of different parameters on the adsorption process. The procedure is as follows: A 150 mL conical flask was applied with a certain amount of adsorbents, placed in a constant temperature water bath shaker and shaken at 120 rpm until equilibrium. The initial pH of the solution was adjusted to the desired value with dilute sodium hydroxide or hydrochloric acid, and samples were taken at certain time intervals. After filtering through a 0.45 μm membrane, the concentration of F^- in the solution was determined by the

fluoride ion selective electrode method. Besides, the concentration of Pb^{2+} in the solution was measured by ICP-OES.

2.6 Effect of TF-Zr on the morphological changes of fluorine and lead in tea garden soil.

2.6.1 Preparation of simulated contaminated soil.

Soil samples were collected from a tea garden soil in Ya'an and followed by cleaning, drying and passing through 60 mesh. Consequently, 2 kg of soil sample was prepared, 4 g of lead nitrate was dissolved in 400 mL of distilled water and poured into the soil to be simulated, allowing uniform mixing just to wet the soil, aged for 40 days under natural conditions, air-dried, ground, sieved and set aside. The basic physicochemical properties of the soils are shown in Table S1.

2.6.2 Soil experimental design.

The effect of the TF-Zr on the F and Pb forms in the soil was investigated in the planted tea garden soil according to the rainy weather condition in Ya'an summer. 100 g of tea garden soil was added in a 250 mL beaker and different amounts of TF-Zr (0.0 g, 0.8 g, 1.4 g, 2.0 g) was also appended in, after uniform mixing, 50 mL of distilled water was added to keep the water content at 50%. Consequently, 0.0428 g of urea, 0.0575 g of potassium dihydrogen phosphate, and 0.0161 g of potassium chloride were added to the obtained mixture respectively. The mixtures were placed and distilled water was added in every one week to ensure the moisture content of the soil. 30 g of soil was sampled every 20 days, air dried, ground and sieved through 60 mesh. Lastly, the pH of the soil was tested, and the different forms of lead and fluorine in soil was also examined by Tessier continuous extraction method and continuous extraction technique (Barathi et al. 2013; Gabarrón et al. 2019).

3. Results and discussion

3.1 Adsorption performance of TF-Zr on Pb^{2+} and F^{-}.

3.1.1 The effect of pH value.

Generally, the pH of the solution is one of the most crucial factors affecting adsorption (Xu et al. 2017). The effect of pH on the adsorption of the prepared TF-Zr on single-component Pb^{2+} at a concentration of 10 mg/L and two-component Pb^{2+} and F^{-} at a concentration of 10 mg/L, respectively, was examined at the pH of 2.5-7.0, The results are shown in Fig. 2(a). Pb^{2+} adsorption experiments were not performed at pH over 7 because Pb^{2+} would form metal precipitates under alkaline conditions, leading to an overestimation of the adsorption capacity of Pb^{2+}. Accordingly, the adsorbed Pb^{2+} increased significantly as the pH increased from 2.5 to 7.0 and remained almost constant thereafter, which was due to the

reduced competition between Pb^{2+} and H^{+} at the same adsorption sites of the adsorbent, and this intense competition occurs at lower pH values.

The existence of F^{-} could greatly influence the adsorption of Pb^{2+} by TF-Zr material. It was found that for the adsorption of single component Pb^{2+} by TF-Zr, the adsorption capacity was 2.08 mg/g and the adsorption equilibrium was reached at pH = 4.5. However, when 10 mg/L F^{-} was added in the solution with 10 mg/L Pb^{+}, the adsorption capacity and the pH at adsorption equilibrium was significantly increased to 4.71 mg/g and 5.5 respectively, which may be attributed to the strong affinity of Zr (IV) on TF-Zr for F^{-} (Huang et al. 2010; Liu et al. 2013) resulting in the enhanced electrostatic attraction between TF-Zr and Pb^{2+} (Cho et al. 2016). In addition, the effect of pH on the adsorption of F^{-} by TF-Zr is tiny (Jiang et al. 2022).

3.1.2 The effect of TF-Zr dosage.

In Fig. 2(b), it was found that with the increase of TF-Zr dosage, the adsorption capacity of TF-Zr on Pb^{2+} increased from 1.91 mg/g to 2.65 mg/g in the single-component system with only Pb^{2+} and from 3.50 mg/g to 4.51 mg/g in the co-existence of 10 mg/L F^{-} and 10 mg/L Pb^{2+}, both of which reached the adsorption equilibrium at the dosage of 0.1 g TF-Zr. The higher TF-Zr dosage provided a large number of adsorption active sites for the whole reaction and increased the surface contact area of the solid-liquid phase in the system. At the same time, the presence of F^{-} had a facilitating effect on the adsorption of Pb^{2+} by TF-Zr, which was attributed to enhanced electrostatic attraction between TF-Zr and Pb^{2+}, similar as the effect of pH.

3.1.3 Pb^{2+} initial concentration and adsorption kinetics.

Commonly, the initial concentration of Pb^{2+} in the solution is an important factor affecting the mass transfer resistance between the aqueous solution and the adsorbent (Arshadi et al. 2017). According to Fig. 3(a), in the initial adsorption stage, the adsorption capacity increased with the increase of initial concentration of Pb^{2+}. Besides, the adsorption reaction of TF-Zr on Pb^{2+} mainly occurred within 20 min, after which the adsorption efficiency gradually declined and slowly tended to equilibrium. At lower initial concentration of Pb^{2+} (3–8 mg/L), there were sufficient number of active sites on the surface of 0.1g TF-Zr for Pb^{2+} adsorption, thus TF-Zr had higher adsorption efficiency for Pb^{2+}. While, at higher initial concentration of Pb^{2+} (12 mg/L), the adsorption efficiency was declined by nearly 4.35%. It was possible that the number of metal ions was more than that of active adsorption sites, leading to the lower adsorption of Pb^{2+} by TF-Zr. As a whole, the adsorption of Pb^{2+} by TF-Zr was limited by the adsorption time and the initial concentration of Pb^{2+}.

The proposed the pseudo-first-order and pseudo-second-order kinetic models were employed to investigate the kinetics of TF-Zr adsorption and analyze the removal mechanism of TF-Zr during the adsorption process. The proposed kinetic models were shown in the following mathematical expressions (1) and (2), respectively:

$q_t = q_e (1-e^{-k_1 t})$ (1)

$q_t = k_2 q_e^2 t/ (1 + k_2 q_e t)$ (2)

Where q_e and q_t are the amount of Pb^{2+} adsorbed at equilibrium and at any time t, k_1 and k_2 are the equilibrium rate constants, and t is the reaction time (min).

The linear fitting of TF-Zr for single-component Pb^{2+} and two-components F^- and Pb^{2+} adsorption are shown in Fig. 3(b) and 3(c). Accordingly, the proposed secondary kinetic results showed a q_e value of 2.364 mg/g for Pb^{2+} adsorption in the absence of F^-. While the q_e value of TF-Zr for Pb^{2+} was 4.608 mg/g in the existence of F^-, which was elevated by 2.224 mg/g in comparison with that without F^- addition. The fitted parameters are shown in Table 1. It was found that the adsorption of Pb^{2+} on TF-Zr fitted the second-order kinetic model well ($R^2 = 0.998$) in the absence of F^-, demonstrating the adsorption of Pb^{2+} on TF-Zr was mainly dominated by chemisorption. Similar results were obtained even if F^- existed. In the meantime, the adsorption of F^- on TF-Zr was consistent with the proposed the pseudo-second-order kinetic model ($R^2 = 0.997$) and was predominant by chemisorption as well. The positive effect of F^- on the adsorption of Pb^{2+} on TF-Zr was also quantified by fitting the q_e values obtained from the the pseudo-first-order and pseudo-second-order kinetic models, where the q_e values in the system containing F^- were higher than the q_e values in the system without F^-.

3.1.4 The effect of different F^- and Pb^{2+} concentration ratios.

As the results mentioned above, the existence of F^- in the adsorption system could significantly improve the adsorption performance of Pb^{2+} by the adsorbent TF-Zr. If the adsorbent would apply in actual soils for simultaneous adsorbing F^- and Pb^{2+}, the concentration ratios of F^- and Pb^{2+} could be an important factor affecting the adsorption performance of TF-Zr. It has been identified that lead and fluorine are present in various forms in actual soli and the concentration of both is a factor that impacts their forms (Gao et al. 2012; Li et al. 2021). Therefore, the effect of the concentration ratio of F^- and Pb^{2+} in aqueous solution on the adsorption characteristics of the adsorbent TF-Zr was investigated. At ambient temperature, F^- and Pb^{2+} can easily react and form PbF_2 sediment. The k_{sp} of PbF_2 refers to 3.3×10^{-8}, and Q_c is calculated by the following Eq. (3):

$Q_c=(F^-)^2\cdot(Pb^{2+})$ (3)

In this study, it was calculated that $Q_c<k_{sp}$ existed in both F^- and Pb^{2+} coexisting solutions, which indicated that there was no precipitation of PbF_2. Meanwhile, the concentrations of Pb^{2+} and F^- in the solutions were examined by ICP-OES and fluorine ion-selective electrode techniques, respectively. As shown in Fig. S1. both F^- and Pb^{2+} existed in the ionic form.

The influence of TF-Zr on Pb^{2+} adsorption under different F^- concentrations (different ratio of F^- and Pb^{2+}) was shown in Fig. 3(d). The adsorption efficiency of TF-Zr on Pb^{2+} increased with the increase of F^- concentration, and the adsorption of Pb^{2+} by the adsorbent tended to equilibrium when the concentration ratio of F^- : Pb^{2+} was 30:10, at which time the removal efficiency of lead was 99.99%. Under this condition, the corresponding adsorption capacity was 5.02 mg/g, which was 2.37 mg/g higher than that in the absence of F^-. it was mainly due to that on the one hand, Pb^{2+} could coordinate with the neighboring phenolic hydroxyl groups on TF-Zr, on the other hand, the electrostatic adsorption of Pb^{2+} could possibly happen on the TF-Zr surface after F^- adsorption (Swain et al. 2019). It was also found that the adsorption efficiency of TF-Zr on F^- increased and then decreased with the increase of F^- concentration, which was attributed to the facts that when the amounts of TF-Zr adsorbent were constant, the active sites were limited. At this time, too much F^- cannot interact with the limited adsorption sites (mainly Zr ions). In conclusion, the presence of F^- favored the adsorption of Pb^{2+} by TF-Zr, which was consistent with the above obtained results.

Table 1
Relevant parameters of the proposed primary and secondary dynamics.

Systems	Pseudo-first-order			Pseudo-second-order		
	$q_e(mg{\cdot}g^{-1})$	K_1	R^2	$q_e(mg{\cdot}g^{-1})$	K_1	R^2
Only Pb^{2+}	1.014	0.014	0.538	2.364	0.222	0.998
(Pb^{2+} and F^-) Pb^{2+}	6.050	0.078	0.925	4.608	0.013	0.934
($Pb^{2+}$and F^-) F^-	2.804	0.050	0.964	5.000	0.056	0.997

3.2 The exploration of adsorption mechanism.

3.2.1 SEM-EDS

The microscopic morphology of TF-Zr was obtained by SEM scanning, finding that the surface of TF-Zr was a non-uniform porous structure (Fig. 4(a)). It was observed that there was nearly no changes in the microscopic morphology of TF-Zr before and after adsorption (Fig. 4(b) and 4(c)).The results of EDS demonstrated that Zr was successfully loaded onto the TF surface (Fig. S2(a)). The signal peaks of Pb and F were observed in Fig. S2(b) and S2(c), respectively, indicating that F and Pb were successfully adsorbed by TF-Zr. Besides, the amount of Pb increased from 1.68 to 1.78 with the addition of F^-, reflecting that the existence of F^- had a facilitating effect on the adsorption of Pb^{2+} by TF-Zr. The Mapping element analysis of TF-Zr was shown in Fig. 4(d-f), revealing that Zr (IV) was uniformly dispersed on the TF surface. In addition, the presence of lead and fluorine elements on the surface of TF-Zr also proved that Pb^{2+} and F^- reacted with the function groups on the surface of TF-Zr.

3.2.2 FT-IR

As shown in Fig. 5(a), the peak at 3400–3500 cm^{-1} is caused by OH stretching vibration, and the peak at 1398 cm^{-1} is caused by OH bending vibration (Liu et al. 2008), indicating that there are a large number of hydroxyl groups on TF surface (Yurtsever et al. 2009). The peaks near 1620 cm^{-1} and 1454 cm^{-1} are attributed to the characteristic peaks of the carbon skeleton structure of the benzene ring, and the peaks near 1040 cm^{-1} are caused by the C-O stretching vibration on the benzene ring. When Zr is loaded onto TF, the peak at 624 cm^{-1} is caused by the tensile vibration of Zr-O-C indicating that Zr is successfully loaded onto TF surface (Prabhu et al. 2015). After the adsorption of Pb^{2+}, the peak of OH bending vibration at 1398 cm^{-1} shifted to 1381 cm^{-1}. Simultaneously, the peaks at 3461 cm^{-1} belonging to OH stretching vibration shifted to 3429 cm^{-1}.These results indicated that the material TF-Zr was able to adsorb Pb^{2+}, which was mainly because Pb^{2+} could react with the hydroxyl groups on the surface of tannins to form stable chelates (Arshadi et al. 2017). Besides, when F^- was added, the shift of OH peak at 1398 cm^{-1} was stronger to 1377 cm^{-1} in comparison with that without F^-, which was possible that the absorption of Pb^{2+} was intensified by the addition of F^-.

3.2.3 XPS

XPS was utilized to determine the surface elemental composition and atomic binding energy of TF and TF-Zr before and after adsorption, through which could reveal the elemental changes and chemical reactions on the surface of the materials TF and TF-Zr (Zou et al. 2019). As shown in Fig. 5(b), for TF-Zr, two peaks of Zr $3d_{3/2}$ and $3d_{5/2}$ appeared at 185.54 eV and 183.19 eV, respectively, indicating that Zr (IV) was successfully loaded on the TF surface. The peak of Pb 4f appeared after the adsorption of Pb^{2+} by TF-Zr (Fig. 5(b)) and the Pb $4f_{5/2}$ and Pb $4f_{7/2}$ peaks with 144.1 eV and 139.2 eV were found in the high resolution spectrum of Pb (Fig.S3), which confirmed the successful adsorption of Pb^{2+} onto the TF-Zr surface. In addition, the TF-Zr with simultaneous adsorption of Pb^{2+} and F^- also showed the Pb 4f peak and F 1s peak (Fig. S3), confirming that Pb^{2+} and F^- could be adsorbed onto the TF-Zr surface. All of these were in accordance with the results of EDS.

To reveal the mechanism of Pb^{2+} adsorbing on TF-Zr, the high resolution spectrum of O element was analyzed (Fig. 5(c)). It was found that three different types of O-linked bonds were existed on TF-Zr at 533.13 eV, 532.42 eV and 530.85 eV, corresponding to C-O, C = O and Zr-O, respectively before adsorption of Pb^{2+}. However, after adsorption of Pb^{2+}, two new peaks appeared at 532.86 eV and 531.82 eV, corresponding to the C-O-Pb and C = O-Pb bond, respectively, while the Zr-O peak was unvaried. Moreover, the increase of the C-O-Pb peak was larger than that of C = O-Pb, indicating that Pb^{2+} was mainly coordinated to the hydroxyl group on the TF-Zr surface during the adsorption. Similar results were observed after the simultaneous adsorption of Pb^{2+} and F^-, which indicated that the addition of F would not change the adsorption mechanism of Pb^{2+} by TF-Zr, but enhance the adsorption capacity of Pb^{2+} by intensifying the electrostatic adsorption between TF-Zr and Pb^{2+}.

It was found from the high resolution spectrum of Zr element (Fig. 5(d)) that the binding energy of Zr had no change before and after adsorption of Pb^{2+}, while the binding energies corresponding to the Zr $3d_{3/2}$ and Zr $3d_{5/2}$ peaks increased from 185.54 eV and 183.19 eV to 185.64 eV and 183.28 eV, respectively with F addition. These results indicated the adsorption process of Pb and F by TF-Zr was independent. Besides, the adsorption of F by TF-Zr was mainly due to the chemical reaction of Zr and F, which decreased the electron cloud density of Zr, resulting in an increase in the binding energy. Similar results were also reported by Wolter and Dou (Dou et al. 2012; Wolter et al. 2011). Meanwhile, the binding energy of the F1s peak was 685.2 eV after the adsorption of F and Pb by TF-Zr, which was closed to that of ZrF_4 with 685.1 eV, also indicating the reaction of F^- with Zr (IV).

3.3 The application of TF-Zr in tea garden soil.

3.3.1 Changes of soil pH.

Soil pH can greatly affect the forms of Pb and F in soil, which can further affect the uptake of F and Pb by tea plants(Yang et al. 2018). In this study, the prepared material TF-Zr with different dosages were added in the tea garden soil to investigate its effect on the soil pH. Importantly, a wet experimental environment was simulated as that of tea garden soil in Ya'an city. The experimental results were indicated in Fig. 6. The addition of TF-Zr could significantly reduce the soil pH at the initial period (20 days). When different amount of TF-Zr(0, 0.8, 1.4, 2.0 g)were added after 20 days, the soil pH was CK (control) > 0.8 > 1.4 > 2.0 g. Specifically, the soil pH with 2.0 g of TF-Zr addition was significantly reduced by 0.57 compared with the control group ($P < 0.05$), which was due to the release of H^+ caused by the weak acidity of bayberry tannins. Subsequently, the soil pH gradually increased in the treatment groups with different amount of TF-Zr addition after 40 and 60 days, while the soil pH in the control group showed insignificant changes. It was proved that the increase of soil pH could be the result of the catalytic effect of hydrogen ions in the esterification reaction (Qiao et al. 2021).

3.3.2 Changes of F forms in soil.

It has been identified that different forms of F exist in tea garden soil, including water-soluble state(water-F), exchangeable state(Ex-F), ferromanganese oxidation state(Fe/Mn-F), organic bound state(Or-F) and residue state(Res-F), and their mobility and biological effectiveness in soil vary greatly(Gan et al. 2021). It was commonly believed that the main forms of F that could migrate from soil to tea trees were the water-soluble and exchangeable states instead of total F (Huang et al. 2020; Zhao et al. 2015). In this work, the effect of TF-Zr applying in tea garden soil on different forms of F was investigate to evaluate the migration ability of fluorine from soil to tea trees. As shown in Fig. 7(a), the content of different forms of F in all treatment groups changed greatly after 60 day' simulating experiment. It was found that the content of water-F and Ex-F gradually and significantly decreased and the content of Fe/Mn-F and Or-F decreased slightly, while the content of Res-F gradually increased. It was obviously found that after 60 days, the water-F and Ex-F could gradually and significantly transform to Res-F in all treatment groups.

Most importantly, the changes of different forms of F with the addition of TF-Zr were quite different from those of the control group. With different amount of TF-Zr addition (0.8-2.0g), the content of various forms of soil F in all the experimental periods changed significantly in comparison with those of the control group, especially the water-F, Ex-F. With the increase of TF-Zr addition from 0.8g to 2.0g, the contents of Water-F and Ex-F in soil decreased gradually and significantly. Especially when 2.0g TF-Zr was added, the water-F and Ex-F deceased by 86.07% and 71.65% after 60 day' simulating experiment, which was 12.54 and 3.80 times higher than those of the control group. Besides, the contents of Res-F increased to 99.03% after 60 day' simulating experiment, which was higher than that of the control group (98.37%). These results showed that adding TF-Zr could promote the transformation of Water-F and Ex-F in soil to Res-F, and the more TF-Zr was added, the more effective Water-F and Ex-F were immobilized. Thus, these findings confirmed that the addition of TF-Zr could effectively prevent fluoride migrating from tea garden soil to tea plants. It was identified that TF-Zr was a natural polymer composite and an organic material. When applied in adsorption of F in soil, it could facilitated the formation of soil agglomerates and provided more adsorption sites on the surface of the soil, resulting in more fluorine to be adsorbed onto the surface of the material and further be immobilized (Erktan et al. 2017). The ability of TF-Zr to reduce the bio-availability of soil fluorine was based on the fact that the Zr(IV) pair on the TF-Zr surface had a strong affinity for F (Wang et al. 2014), which could make the Zr-F structure easily formed.

3.3.3 Changes of Pb forms in soil.

The forms of heavy metals in soil can greatly affect the soil environmental quality and uptake of heavy metals by plants (Xia et al. 2021). It has been identified that the exchangeable state is considered to be the most readily available for plants uptake in soil, while the residual state is extremely stable, which can be tightly bound to the mineral lattice and within the crystalline oxide and is difficult to release into the soil environment (Sut-Lohmann et al. 2022). Therefore, enhancing the transformation of exchangeable state of heavy metals to residual state has been regarded as a feasible and effective way to reduce the pollution and threat of heavy metals in soil. In this work, the effect of TF-Zr applying in tea garden soil on different forms of Pb was investigated to evaluate the immobilization ability and remediation performance of soil Pb. In order to better observe the influence of TF-Zr on different forms of Pb in soil, a certain amount of exogenous lead (about 1250 mg/kg dry soil) was added to the original soil in this study. Therefore, the content of Ex-Pb in the soil was relatively high at the initial experimental stage, accounting for 77.36% of the total Pb content. As shown in Fig. 7(b), the content of different forms of Pb in all treatment groups changed greatly after 60 days' simulating experiment, especially Ex-Pb and Res-Pb. It was found that the content of Ex-Pb gradually and significantly decreased, while the content of Res-F gradually and significantly increased, indicating the gradual and significant transformation of Ex-Pb to Res-Pb in all treatment groups with 60 days' experiment.

Besides, it was obviously found that the changes of different forms of Pb with the addition of TF-Zr were quite different from those of the control group. After 20 days' experiment, the Ex-Pb content decreased by 51.88%, 56.19% and 63.95% with the addition of 0.8, 1.4 and 2.0 g TF-Zr respectively, which was 2.08, 2.26 and 2.57 times higher than that of the control group (without TF-Zr addition). Meanwhile, the Res-Pb

content in the total Pb in soil with the addition of 0.8, 1.4 and 2.0g TF-Zr accounted for 22.01%, 23.30% and 33.11% after 20 days respectively, which increased by 18.39%,19.68% and 29.49% compared with the control group. These results indicated that the addition of TF-Zr could significantly accelerate the transformation of Ex-Pb to Res-Pb in soil and the more TF-Zr was added, the faster Ex-Pb was transformed to Res-Pb. After 60 days, the decrease of Ex-Pb with 2.0g TF-Zr addition was as high as 751.25 mg/g and the increase of Res-Pb reached to 471.90 mg/g. Moreover, the changes of Fe/Mn-Pb and Or-Pb contents were similar with that of Ex-Pb, but it was not as obvious as the changes of Ex-Pb content, which was possibly due to the relative lower content of Fe/Mn-Pb and Or-Pb in comparison with Ex-Pb. In conclusion, the application of TF-Zr in tea garden soil could promote and accelerate the transformation of Ex-Pb to Res-Pb, and also promote the transformation of other forms of Pb to Res-Pb, which could effectively prevent the pollution of Pb in soil and control the migration of Pb to tea trees. The ability of TF-Zr to reduce the pollution and threat of Pb in soil was based on the complexation of hydroxyl group on the surface of TF-Zr with the Ex-Pb, in which the highly reactive Ex-Pb could be converted to the most stable form (Res-Pb).

3.3.4 The analysis of Pearson correlation.

The immobilization of Pb and F in soil by application of the material TF-Zr could be affected by many factors, such as soil pH, TF-Zr dosage and different forms of Pb and F. The Pearson correlation analysis were carried out to reveal the potential important factors, as shown in Tables 2 and 3. During the whole 60 days' experiment, the soil pH value was significantly correlated with TF-Zr dosage (positive) and different forms of Pb and F (positive or negative) ($P < 0.01$) only with 20 days (table S2-1, S2-2 and S3-1, S3-2). It was mainly because the excess addition of TF-Zr could release H + in soil at the initial periods, which would cause the decrease of soil pH and affect the existing forms of Pb and F. However, the influence of TF-Zr addition was insignificant on soil pH thereafter.

Table 2
Pearson correlation analysis of TF-Zr dosage, pH, different fractions of fluorine at different test days.

	Dosage of TF-Zr	**pH**	**Water-F**	**Ex-F**	**Fe/Mn-F**	**Or-F**	**Res-F**
Dosage of TF-Zr	1						
pH	-0.133	1					
Water-F	**-0.896****	-0.315	1				
Ex-F	**-0.825****	-0.355	**0.918****	1			
Fm-F	**-0.816****	-0.245	**0.924****	0.697*	1		
Or-F	-0.628**	-0.315	-0.684*	**0.917****	-353	1	
Res-F	**0.894****	0.324	**-0.999****	**-0.936****	**0.904****	**-0.718****	1

**. $P \leq 0.01$, the correlation was significant. *. $P \leq 0.05$, the correlation was significant.

Table 3
Pearson correlation analysis of TF-Zr dosage, pH, different fractions of lead at different test days

	Dosage of TF-Zr	pH	Ex-Pb	Car-Pb	Fe/Mn-Pb	Or-Pb	Res-Pb
Dosage of TF-Zr	1						
pH	-0.133	1					
Ex-Pb	**-0.795****	-0.440	1				
Ca-Pb	-0.431	-0.546	**0.847****	1			
Fm-Pb	**-0.610***	0.442	0.114	-0.422	1		
Or-Pb	**-0.808****	-0.457	**0.995****	**0.796****	0.188	1	
Res-Pb	**0.796****	0.424	**-0.999****	**-0.857****	-0.100	**-0.991****	1

**. $P \leq 0.01$, the correlation was significant. *. $P \leq 0.05$, the correlation was significant.

Besides, the TF-Zr dosage showed a significantly negative correlation ($P < 0.01$) with Water-F, Ex-F, Fe/Mn-F, Ex-Pb and Or-Pb and a significantly positive correlation ($P < 0.01$) with Res-F and Res-Pb, which indicated the addition of TF-Zr could reduce the active forms of F and Pb and increase the stable form of F and Pb (Table 2 and 3). These findings were in line with the changes of different forms of soil F and Pb above mentioned. From the correlation analysis of different forms of F, it was obvious that Water-F, Ex-F and Fe/Mn-F were significantly positive correlation ($P < 0.01$) with each other, while they were negatively correlated with Res-F suggesting that Water-F, Ex-F and Fe/Mn-F could transform to Res-Pb. The correlation analysis results of different forms of Pb were similar with those of F. The Ex-Pb, Car-Pb and Or-Pb were significantly positive correlation ($P < 0.01$) with each other, while they were negatively correlated with Res-Pb suggesting that Ex-Pb, Car-Pb and Or-Pb could transform to Res-Pb. However, the Fe/Mn-Pb had little correlation with other forms of Pb. This was probably due to insignificant changes of Fe/Mn-Pb after adding of different of TF-Zr during the whole experimental periods.

4. Conclusion

In this study, the adsorption properties of TF-Zr on Pb^{2+} and F^- in water were evaluated. It was found that TF-Zr had a good adsorption capacity for both Pb^{2+} and F^-, which was because Pb^{2+} and F- was effectively combined with hydroxyl group and Zr ion on the surface of TF-Zr. Besides, the presence of F^- promoted the adsorption of Pb^{2+} by TF-Zr owing to the enhancement of electrostatic effect. Moreover, it was identified that when the TF-Zr material was applied to tea garden soil, the forms of Pb and F in soil changed greatly from highly active state to the most stable residual state, which indicated that the material could effectively and simultaneously prevent the pollution of Pb and F in soil and control their migration to tea trees.

Declarations

Author contributes

This manuscript is a joint effort by all the authors. Xiaolu Huang mainly did some experiments and wrote this paper, Mei Zhang, Minghui Wang, and Zhuoyu Wen participated in the drawing of the paper, and Yamei Jiang, Yunhao Sui did the experiments, Xiaoting Li, Jun Ma and Yang Liao proposed the experimental ideas and methods, guided the writing and revision of this paper.

Acknowledgement

This work was supported by the National Natural Science Foundation of China (41641010), the Foundation of Sichuan Science & Technology Committee (2020YFH0162) and Innovation Project and Training Program for College Students (X202210636212).

Conflict of interest

The authors declare that there is no conflict of interest to this work.

Consent to participant

All the authors have given approval for the final version of manuscript.

References

1. Arshadi, M., Abdolmaleki, M. K., Mousavinia, F., Foroughifard, S., & Karimzadeh, A. (2017). Nano modification of NZVI with an aquatic plant Azolla filiculoides to remove Pb(II) and Hg(II) from water: Aging time and mechanism study. *Journal of Colloid and Interface Science*, 486, 296-308.
2. Barathi, M., Santhana Krishna Kumar, A., & Rajesh, N. (2013). Efficacy of novel Al–Zr impregnated cellulose adsorbent prepared using microwave irradiation for the facile defluoridation of water. *Journal of Environmental Chemical Engineering*, 1(4), 1325-1335.
3. Cao, J., Zhao, Y., & Liu, J. (1997). Brick tea consumption as the cause of dental fluorosis among children from Mongol, Kazak and Yugu populations in China. *Food and Chemical Toxicology*, 35(8), 827-833.
4. Cho, D. W., Jeon, B. H., Jeong, Y., Nam, I. H., Choi, U. K., Kumar, R., & Song, H. (2016). Synthesis of hydrous zirconium oxide-impregnated chitosan beads and their application for removal of fluoride and lead." *Applied Surface Science*, 372, 13-19.
5. Dou, X. M., Mohan, D., Pittman, C. U., & Yang, S. (2012). Remediating fluoride from water using hydrous zirconium oxide. *Chemical Engineering Journal*, 198-199, 236-245.
6. Erktan, A., Balmot, J., Merino-Martín, L., Monnier, Y., Pailler, F., Coq, S., Abiven, S., Stokes, A., & Le Bissonnais, Y. (2017). Immediate and long-term effect of tannins on the stabilization of soil aggregates. *Soil Biology and Biochemistry*, 105, 197-205.

7. Fan, C. F., Yin, N. Y., Cai, X. L., Du, X., Wang, P. F., Liu, X. T., Li, Y P., Chang, X. H., Du, H. L., Ma, J. N., & Cui, Y. S. (2022). Stabilization of fluorine-contaminated soil in aluminum smelting site with biochar loaded iron-lanthanide and aluminum-lanthanide bimetallic materials. *Journal of Hazardous Materials*, 426, 128072.
8. Gabarrón, M., Zornoza, R., Martínez-Martínez, S., Muñoz, V. A., Faz, Á., & Acosta, J. A. (2019). Effect of land use and soil properties in the feasibility of two sequential extraction procedures for metals fractionation. *Chemosphere*, 218, 266-272.
9. Gan, C. D., Jia, Y. B., & Yang, J. Y. (2021). Remediation of fluoride contaminated soil with nano-hydroxyapatite amendment: Response of soil fluoride bioavailability and microbial communities. *J Hazard Mater*, 405, 124694.
10. Gao, H. J., Zhang, Z. Z., & Wan, X. C. (2012). Influences of charcoal and bamboo charcoal amendment on soil-fluoride fractions and bioaccumulation of fluoride in tea plants. *Environmental Geochemistry & Health*, 34(5), 551-562.
11. Guo, Y. L., Wang, G., Luo, D., Ge, H. L., Wang, G. F., Chen, J. H., & Luo, Z. Y. (2011). Environmental quality of lead, cadmium, arsenic, chromium, mercury, copper and fluorine in the soil of Tieguanyin Tea Garden in Fujian Province. *Chinese Journal of Eco-Agriculture*, 19(03), 676-681.
12. Han, W. Y., Zhao, F. J., Shi, Y. Z., Ma, L. F., & Ruan, J. Y. (2006). Scale and causes of lead contamination in Chinese tea. *Environmental Pollution*, 139(1), 125-132.
13. Havugimana, E., Bhople, B. S., Kumar, A., Byiringiro, E., & Kumar, A. (2017). Soil Pollution-Major Sources and Types of Soil Pollutants.
14. Huang, C. Y., Zhang, H., Zeng, W. H., Ma, J., Zhao, S. L., Jiang, Y. F., Huang, C. R., Mao, H., & Liao, Y. (2020). Enhanced fluoride adsorption of aluminum humate and its resistance on fluoride accumulation in tea leaves. *Environmental Technology*, 41(3), 329-338.
15. Huang, X., Wang, Y., Liao, X., & Shi, B. (2010). Adsorptive recovery of Au^{3+} from aqueous solutions using bayberry tannin-immobilized mesoporous silica. *J Hazard Mater*, 183(1-3), 793-8.
16. Jiang, Y. M., Li, C. Q., Huang, X. L., Hao, B. C., Li, X. T., Ma, J., Mao, H., Zhao, S. L., & Liao, Y. (2022). Zirconium loaded on tannin foam for efficient adsorptive removal of fluoride at low concentration in a wide pH range. *Desalination and Water Treatment*, 250, 159-171.
17. Jin, C. W., Zheng, S. J., He, Y. F., Zhou, G. D., & Zhou, Z. X. (2005). Lead contamination in tea garden soils and factors affecting its bioavailability. *Chemosphere*, 59(8), 1151-1159.
18. Li, H. H., Liu, Y. T., Tang, S. Y., Yu, Z. C., Cai, X. Z., Xu, S. P., Chen, Y. H., Wang, M. K., & Wang, G. (2021). Mechanisms for potential Pb immobilization by hydroxyapatite in a soil-rice system. *Science of The Total Environment*, 783, 147037.
19. Liu, B. J., Wang, D. F., Yu, G. L., & Meng, X. H. (2013). Removal of F− from aqueous solution using Zr(IV) impregnated dithiocarbamate modified chitosan beads. *Chemical Engineering Journal*, 228, 224-231.
20. Liu, H. L., Sun, X. F., Yin, C. Q., & Hu, C. (2008). Removal of phosphate by mesoporous ZrO2. *J Hazard Mater*, 151(2-3), 616-22.

21. Long, H., Jiang, Y. M., Li, C. Q., Liao, S. T., & Liao, Y. (2021). Effect of urea feeding on transforming and migrating soil fluorine in a tea garden of hilly region. *Environmental Geochemistry and Health*(2–3).
22. Luo, Y., Yuan, H., Zhao, J., Qi, Y., Cao, W. W., Liu, J. M., Guo, W., & Bao, Z. H. (2021). Multiple factors influence bacterial community diversity and composition in soils with rare earth element and heavy metal co-contamination. *Ecotoxicology and Environmental Safety*, 225, 112749.
23. Peng, J. Y., Chen, Y. A., Xia, Q., Rong, G. Z., & Zhang, J. Q7. (2021). Ecological risk and early warning of soil compound pollutants (HMs, PAHs, PCBs and OCPs) in an industrial city, Changchun, China. *Environmental Pollution*, 272, 116038.
24. Prabhu, S. M., & Meenakshi, S. (2015). Defluoridation of water using synthesized Zr(IV) encapsulated silica gel/chitosan biocomposite: Adsorption isotherms and kinetic studies. *Desalination and Water Treatment*, 53(13), 3592-3603.
25. Qi, X., Yin, H., Zhu, M. H., Yu. X. L., Shao, P. L., & Dang, Z. (2022). MgO-loaded nitrogen and phosphorus self-doped biochar: High-efficient adsorption of aquatic Cu^{2+}, Cd^{2+}, and Pb^{2+} and its remediation efficiency on heavy metal contaminated soil. *Chemosphere*, 294, 133733.
26. Qiao, D. W., Yao, J., Song, L. J., & Yang, J. Y. (2021). Migration of leather tannins and chromium in soils under the effect of simulated rain. *Chemosphere*, 284, 131413.
27. Qin, F. X., Wu, D., Huang, X. F., Yang, Y., Xu, K., & Pang, W. P. (2014). Fluoride morphology and distribution characteristics of soil in tea gardens in high fluoride affected areas. *Chinese environmental science*, 34(11), 2859-2865.
28. Ruan, J. Y., Ma, L. F., Shi, Y. Z., & Han, W. Y. (2003). Uptake of fluoride by tea plant (Camellia sinensis L) and the impact of aluminium. *Journal of the Science of Food & Agriculture*, 83(13), 1342–1348.
29. Singh, S., German, M., Chaudhari, S., & Sengupta, A. K. (2020). Fluoride removal from groundwater using Zirconium Impregnated Anion Exchange Resin. *Journal of Environmental Management*, 263, 110415.
30. Sun, J. W., Yu, R. L., Yan, Y., Hu, G. G., Qiu, Q. J., Jiang, S. Y., Cui, J. Y., Wang, X. M., & Ma, C. (2020). Isotope tracers for lead and strontium sources in the Tieguanyin tea garden soils and tea leaves. *Chemosphere*, 246, 125638.
31. Sut-Lohmann, M., Ramezany, S., Kästner, F., Raab, T., Heinrich, M., & Grimm, M. (2022). Using modified Tessier sequential extraction to specify potentially toxic metals at a former sewage farm. *Journal of Environmental Management*, 304, 114229.
32. Swain, S. K., Patel, S. B., Panda, A. P., Patnaik, T., & Dey, R. K. (2019). Pea (Pisum sativum L.) peel waste carbon loaded with zirconium: study of kinetics, thermodynamics and mechanism of fluoride adsorption. *Separation Science and Technology*, 54(14), 2194-2211.
33. Wang, J., & Chen, C. (2014). Chitosan-based biosorbents: Modification and application for biosorption of heavy metals and radionuclides. *Bioresource Technology: Biomass, Bioenergy, Biowastes, Conversion Technologies, Biotransformations, Production Technologies*.

34. Wang, J., Lin, X. Y., Luo, X. G., & Long, Y. F. (2014). A sorbent of carboxymethyl cellulose loaded with zirconium for the removal of fluoride from aqueous solution. *Chemical Engineering Journal*, 252, 415-422.
35. Wolter, S. D., Piascik, J. R., & Stoner, B. R. (2011). Characterization of plasma fluorinated zirconia for dental applications by X-ray photoelectron spectroscopy. *Applied Surface Science*, 257(23), 10177-10182.
36. Xia, Y., Li, Y., Sun, Y. T., Miao, W., & Liu, Z. G. (2021). Co-pyrolysis of corn stover with industrial coal ash for in situ efficient remediation of heavy metals in multi-polluted soil. *Environmental Pollution*, 289, 117840.
37. Xu, J. C., Wang, S. Q., Yao, T. S., She, X. S., & Gan, Z. T. (2022). Vertical Distributions and Bioavailabilities of Heavy Metals in Soil in An-Tea Plantations in Qimen County, China. *Processes*, 10(4), 664.
38. Xu, Q. H., Wang, Y. L., Jin, L. Q., Wang, Y., & Qin, M. H. (2017). Adsorption of Cu (II), Pb (II) and Cr (VI) from aqueous solutions using black wattle tannin-immobilized nanocellulose. *Journal of Hazardous Materials*, 339, 91-99.
39. Yang, X. D., Ni, K., Shi, Y. Z., Yi, X. Y., Zhang, Q. Ff., Fang, L., Ma, L. F., & Ruan, J. Y. (2018). Effects of long-term nitrogen application on soil acidification and solution chemistry of a tea plantation in China. *Agriculture, Ecosystems & Environment*, 252, 74-82.
40. Yurtsever, M., & Şengil, İ. A. (2009). Biosorption of Pb(II) ions by modified quebracho tannin resin. *Journal of Hazardous Materials*, 163(1), 58-64.
41. Zhang, H. Y., Jiang, L. B., Wang, H., Li, Y., Chen, J., Li, J. Y., Guo, H., Yuan, X. Z., & Xiong, T. (2022). Evaluating the remediation potential of MgFe2O4-montmorillonite and its co-application with biochar on heavy metal-contaminated soils. *Chemosphere*, 299, 134217.
42. Zhang, J., Yang, R. D., Li, Y. C., Peng, Y. S., Wen, X. F., & Ni, X. R. (2020). Distribution, accumulation, and potential risks of heavy metals in soil and tea leaves from geologically different plantations. *Ecotoxicology and Environmental Safety*, 195, 110475.
43. Zhang, W. H., Yan, Y., Yu, R. L., & Hu, G. R. (2021). The sources-specific health risk assessment combined with APCS/MLR model for heavy metals in tea garden soils from south Fujian Province, China. *CATENA*, 203, 105306.
44. Zhao, S. L., Liu, Y., Ma, J., Mao, H., Lan, T., Jiang, Y. F., & Liao, Y. (2015). Influence of fertilizers on fluoride accumulation in tea leaves & its remediation using polyphenol-Ce adsorbents. *RSC Advances*, 5(8).
45. Zhuang, Z., Mi, Z. D., Kong, L. X., Wang, Q., Schweiger, A. H., Wan, Y. N., & Li, H. F. (2022). Accumulation of potentially toxic elements in Chinese tea (Camellia sinensis): Towards source apportionment and health risk assessment. *Science of The Total Environment*, 851, 158018.
46. Zou, L. Z., Shao, P. H., Zhang, K., Yang, L. M., You, D., Shi, H., Pavlostathis, S. G., Lai, W. Q., Liang, D. H., & Luo, X. B. (2019). Tannic acid-based adsorbent with superior selectivity for lead(II) capture: Adsorption site and selective mechanism. *Chemical Engineering Journal*, 364, 160-166

Figures

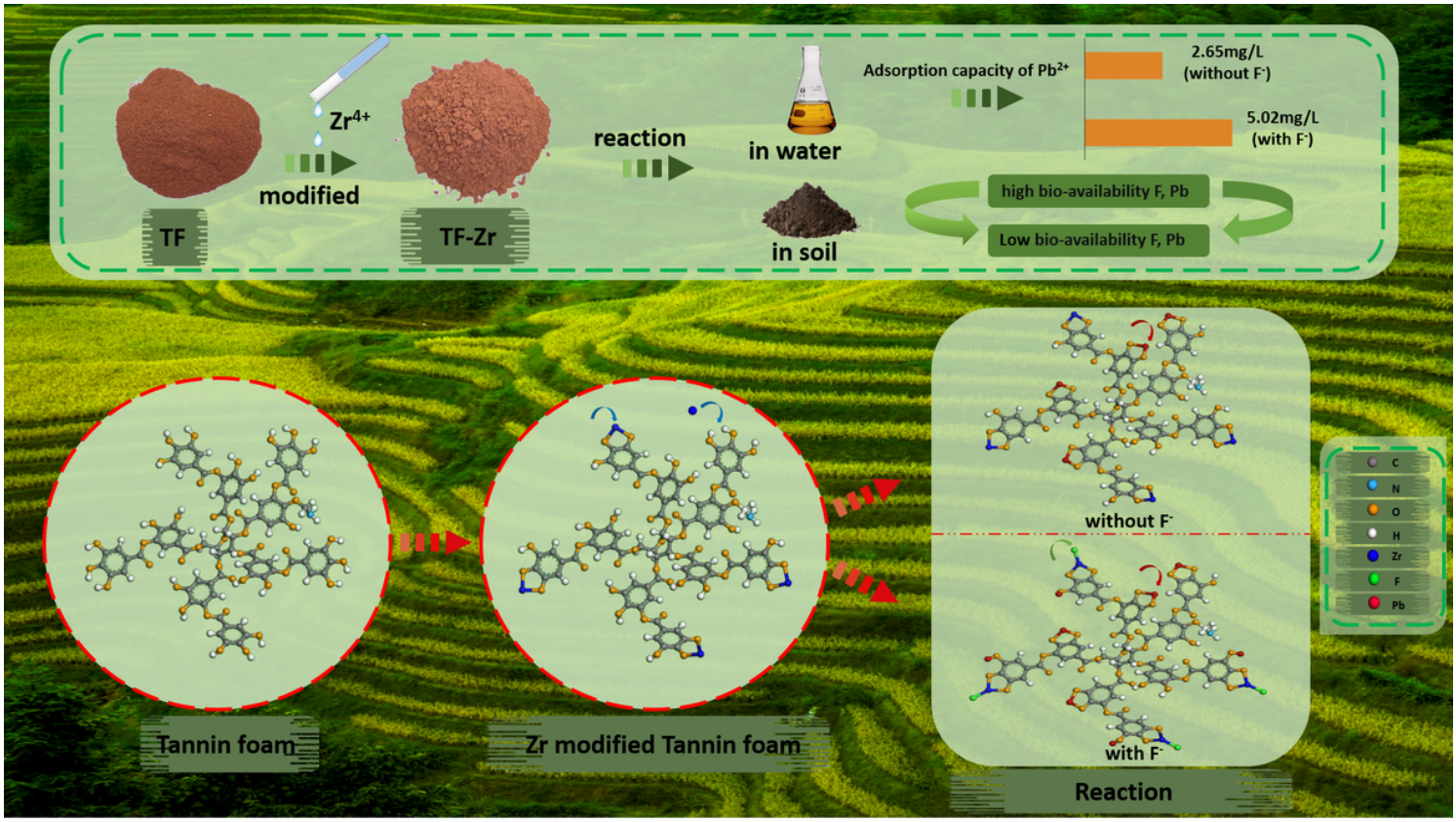

Figure 1

The strategy and principle for simultaneous immobilization of F and Pb in water or in soil

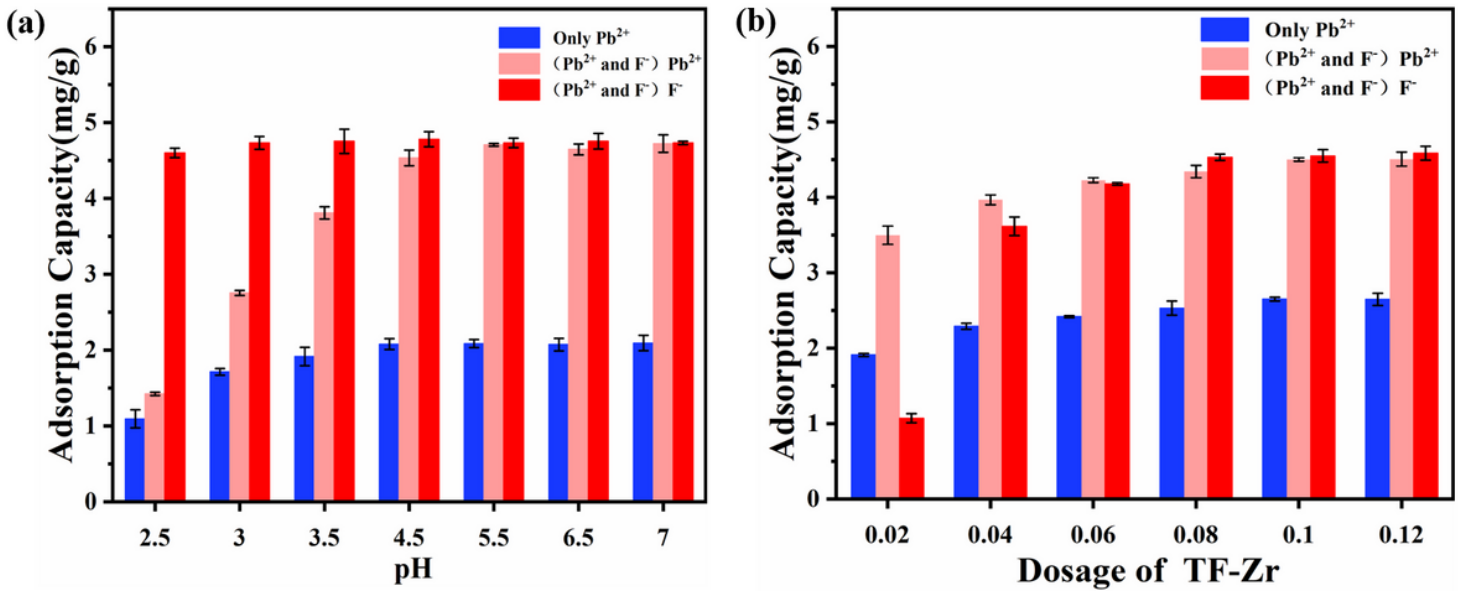

Figure 2

The effect of pH(a) and TF-Zr dosage(b) on adsorption of single-component Pb^{2+} (10 mg/L) and two-component Pb^{2+} (10 mg/L) and F- (10 mg/L).

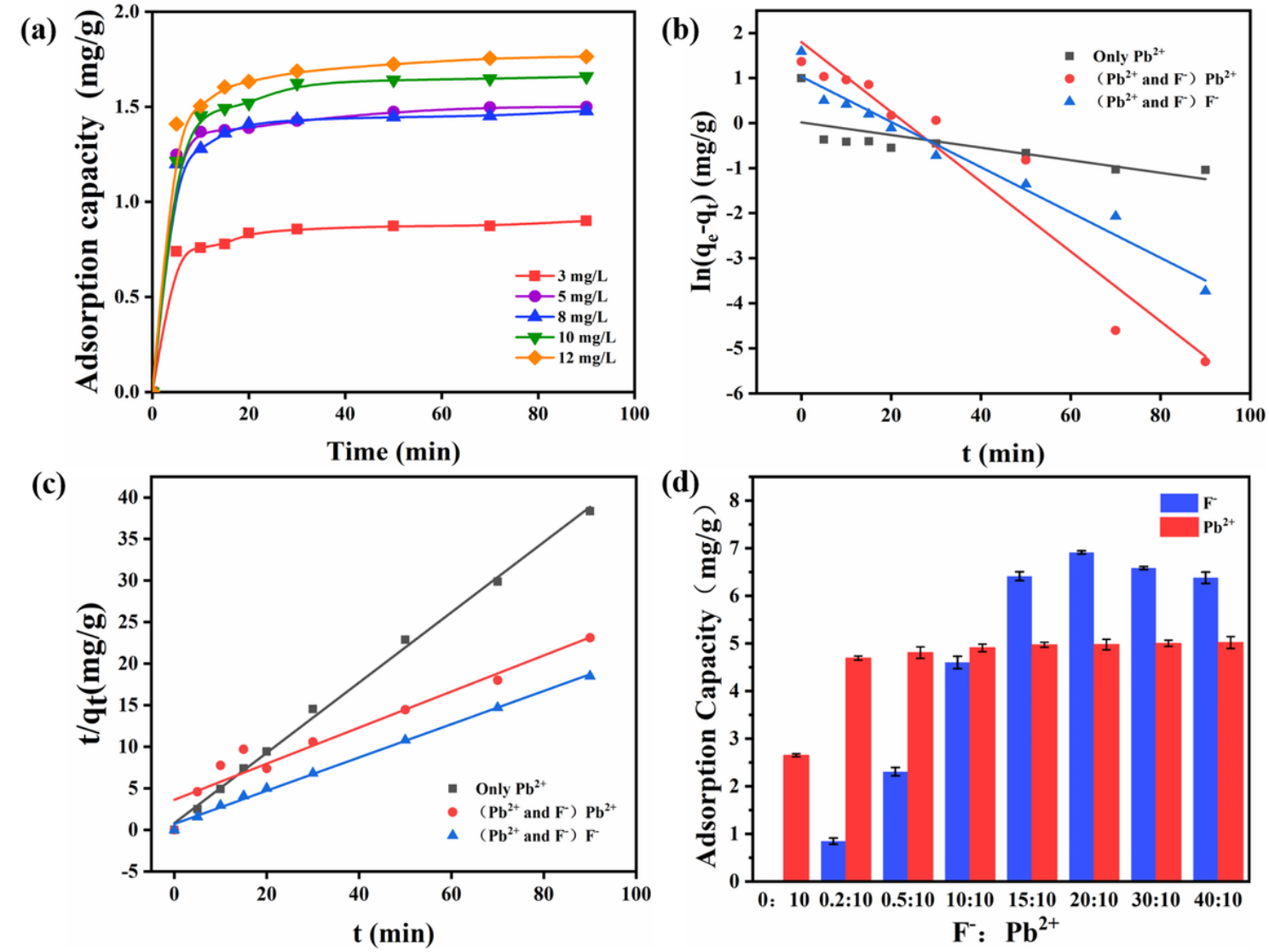

Figure 3

(a)The effect of initial Pb^{2+} concentration on the adsorption of Pb^{2+} by 0.1g TF-Zr; The curves of (b) proposed primary dynamic and (c) proposed secondary dynamic; (d)Adsorption capacity of TF-Zr on Pb^{2+} and F^- under different concentration ratios of F^- and Pb^{2+}.

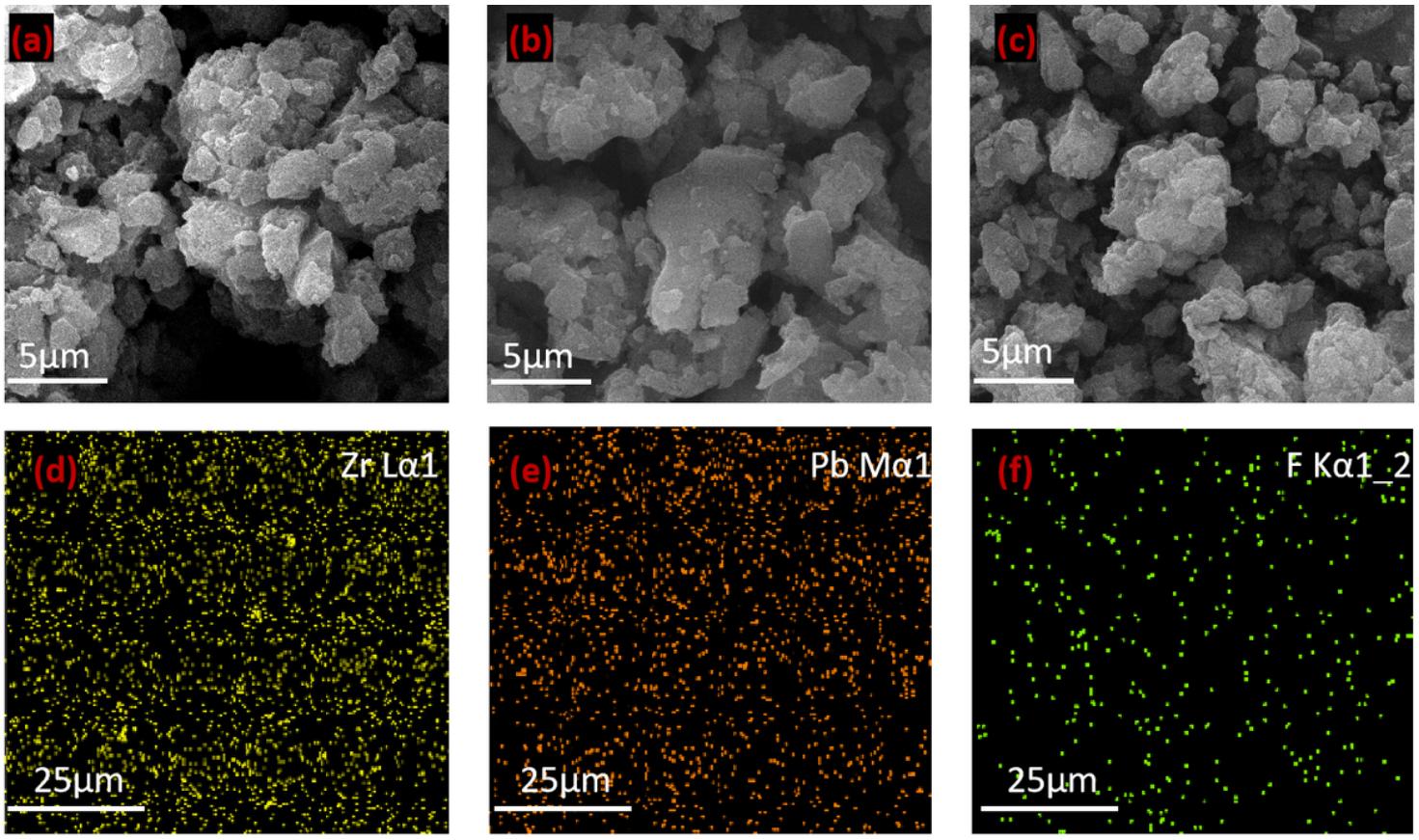

Figure 4

SEM of TF-Zr before and after adsorption (a) TF-Zr, (b) TF-Zr adsorbed lead, (c) TF-Zr adsorbed both fluorine and lead and Mapping of TF-Zr adsorbed both fluorine and lead, (d) Zr, (e) Pd (f) F.

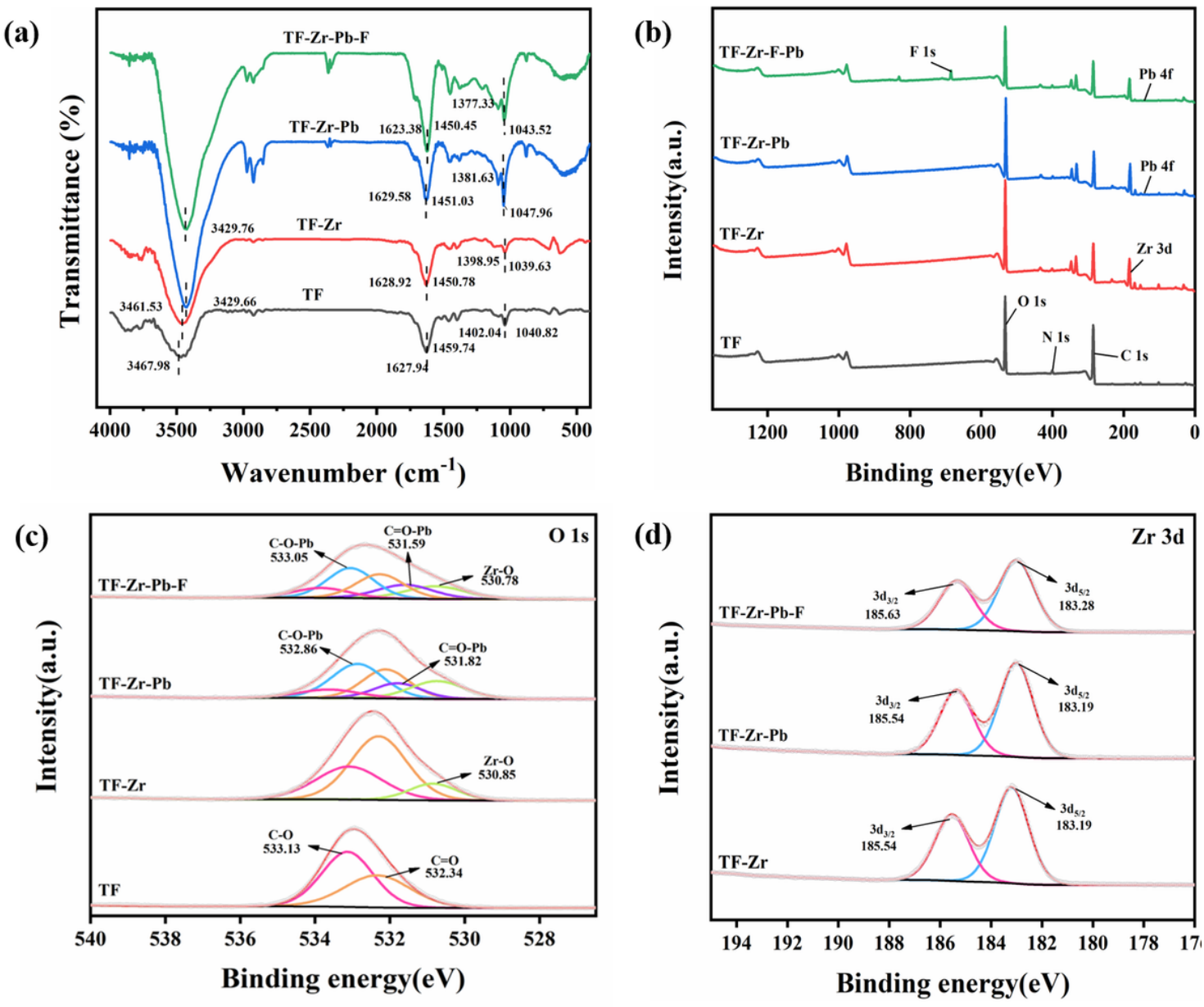

Figure 5

(a) FT-IR; (b) XPS spectra of TF and TF-Zr before and after adsorption; (c) XPS O 1s of TF and TF-Zr before and after TF-Zr adsorption; (d)XPS Zr 3d before and after TF-Zr adsorption.

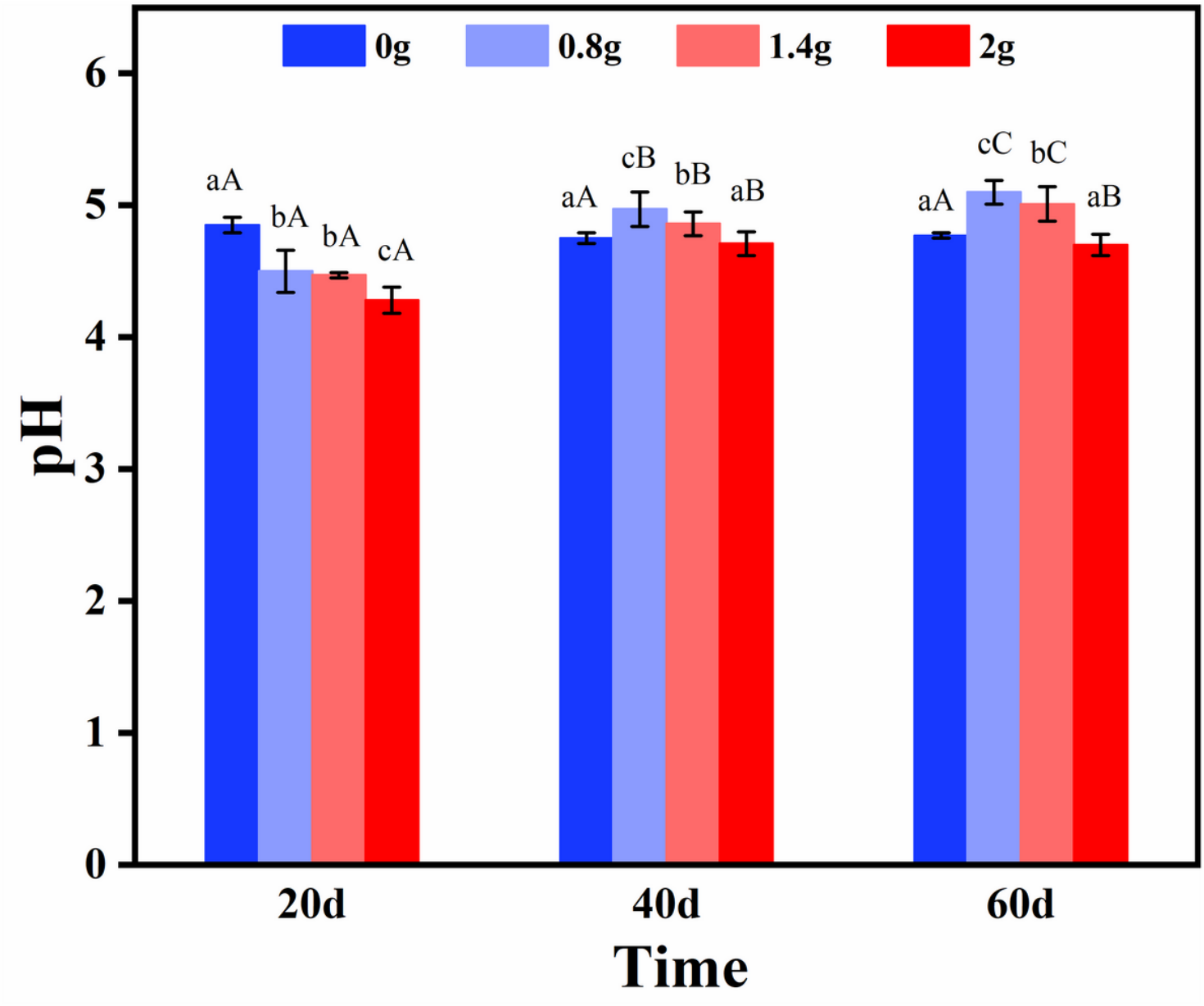

Figure 6

The soil pH with different TF-Zr dosages at different experimental days.

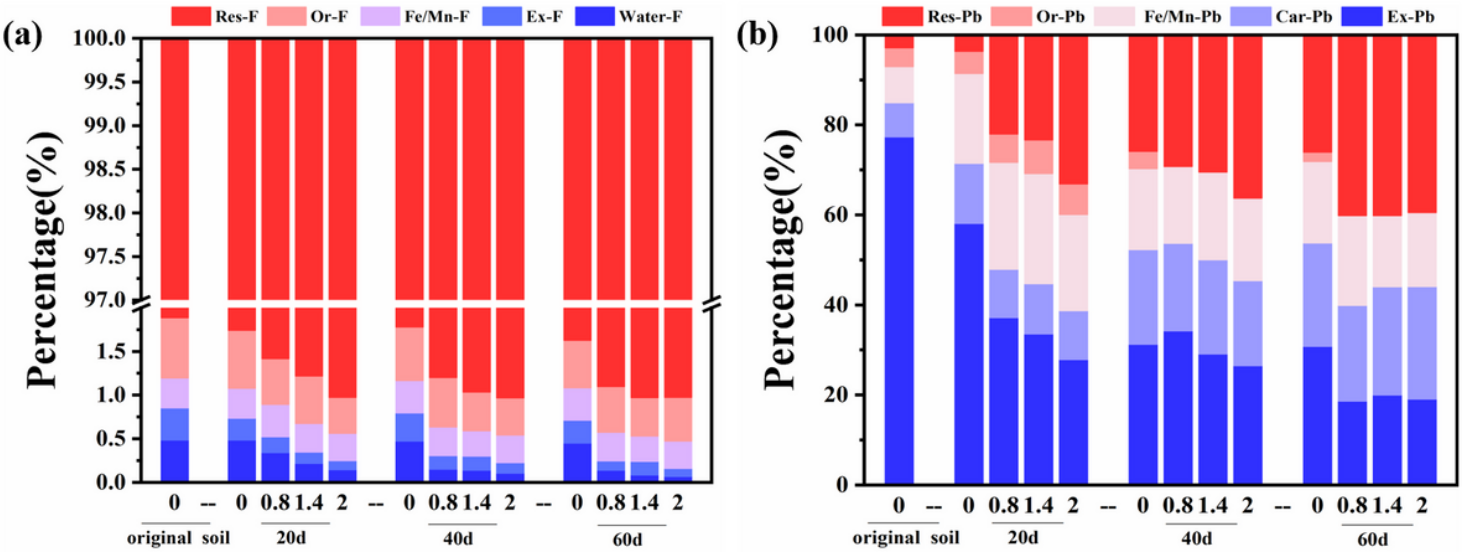

Figure 7

(a) The changes of different forms of F in soil with different amount of TF-Zr addition. (b) The changes of different forms of Pb in soil with different amount TF-Zr addition.

Supplementary Files

This is a list of supplementary files associated with this preprint. Click to download.

- supporting.docx